Cytochrome *c* - cyclo[6]aramide complex as supramolecular catalyst in methanol

Wang Pan,‡[a] Lijun Mao,‡[a] Mingsong Shi,[a] Yonghong Fu,[a] Xiaomin Jiang,[a] Wen Feng,[a] Youzhou He,[b] Dingguo Xu*[a] and Lihua Yuan*[a]

[a]*College of Chemistry, Key Laboratory for Radiation Physics and Technology of Ministry of Education, Institute of Nuclear Science and Technology, Sichuan University, Chengdu 610064, China. E-mail: lhyuan@scu.edu.cn, dgxu@scu.edu.cn; Fax: +86-28-85418755; Tel: +86-28-85412890*

[b]*Chongqing Key Laboratory of Catalysis & Functional Organic Molecules, College of Environment and Resources, Chongqing Technology and Business University, Chongqing 400067, China*

Electronic Supplementary Information

Contents

1 General information

All chemicals were obtained from commercial suppliers and were used as received without further purification unless otherwise noted, for example the substrates **3a** (benzhydrol), **3b** (4,4'-difluorobenzhydrol), and **3c** (4,4'-dimethoxybenzhydrol). CH_2Cl_2 was dried over CaH_2. Solvents for extraction were reagent grade. $CDCl_3$ was from Cambridge Isotope Laboratories (CIL) and acetone-d_6 was supplied by Aldrich.

^1H NMR and ^{13}C NMR spectra were recorded on Bruker AVANCE AV II-400 MHz (^1H: 400 MHz; ^{13}C: 101 MHz). Chemical shifts are reported in δ values in ppm using tetramethylsilane (TMS) as internal standard and coupling constants (J) are denoted in Hz. Multiplicities are denoted as follows: s = singlet, d = doublet, t = triplet, and m = multiplet. High resolution mass spectrometer (HRMS) data were obtained by WATERS Q-TOF Premier. UV-vis spectra were measured by SHIMADZU UV-2450. CD spectra were measured by Jasco J-1500. Raman spectra were measured by LabRAM HR spectrometer (HORIBA Jobin Yvon S.A.S.). Oxidation reaction data were recorded on HPLC, Diamonsil C18, 25 ℃, H_2O/methanol = 3/7, 1.0 mL/min. MALDI-TOF MS spectra were recorded on Bruker Autoflex III MS spectrometer (DHAP as the matrix, methanol as the solvent).

2 Synthesis of compounds 1, 2, 3d, and 3e

Cyclo[6]aramide **1** was synthesized following a literature procedure.[S1] Cyclo[6]aramide **2** was only used for calculation purpose.

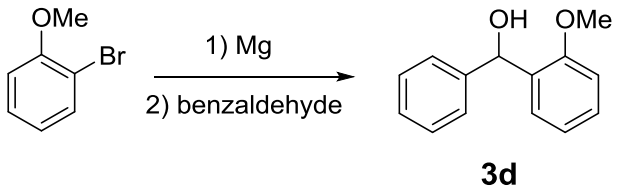

3d

Scheme S1. Synthetic route of compound **3d** (2-methoxyphenyl(phenyl)methanol).

To a mixture of 2-bromoanisole (200 mg, 1.07 mmol) and polished magnesium (390 mg, 1.60 mmol) in dry THF was added a grain of I_2. The solution was stirred at room temperature for 1.0 h. Then, benzaldehyde (114 mg, 1.07 mmol) was added to the solution under ice bath. The temperature was allowed to rise to 66 ℃ for 2.0 h. Subsequently, the solution was cooled to room temperature followed by adding 5.0

mL saturated NH_4Cl solution. The solvent was then removed under reduced pressure and the resulting product was suspended in CH_2Cl_2 (10 mL), washed with H_2O (10 mL). After drying of the organic phase over Na_2SO_4 and evaporation of the solvent, the residue was purified by filtration column (SiO_2, hexane/AcOEt = 5/1, v/v) affording **3d** as colorless oil (183 mg, 0.86 mmol, 80%). ^{1}H NMR (400 MHz, Acetone-d_6) δ 7.28 (dd, J = 7.5, 1.6 Hz, 2H), 7.21 (td, J = 8.0, 1.7 Hz, 2H), 6.93 (d, J = 8.1 Hz, 2H), 6.89 (t, J = 7.5 Hz, 2H), 6.41 (d, J = 4.9 Hz, 1H), 4.34 (s, 1H), 3.76 (s, 6H); ^{13}C NMR (101 MHz, Acetone-d_6) δ 157.00, 146.16, 134.53, 128.80, 128.61, 127.58, 127.36, 121.20, 111.28, 69.93, 55.67; ESI-HRMS (m/z) calcd. for $C_{14}H_{14}O_2$ $[M+Na]^+$ 237.2495, found 237.0859.

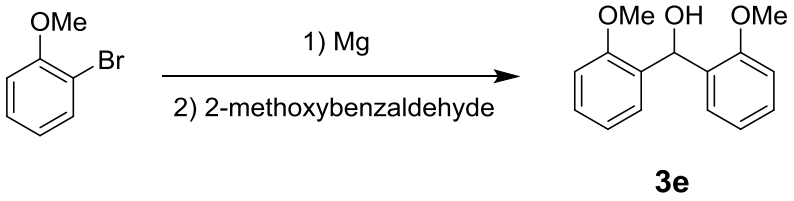

3e

Scheme S2. Synthetic route of compound **3e** (bis(2-methoxyphenyl)methanol).

To a mixture of 2-bromoanisole (200 mg, 1.07 mmol) and polished magnesium (390 mg, 1.60 mmol) in dry THF was added a grain of I_2. The solution was stirred at room temperature for 1.0 h. Then, 2-methoxybenzaldehyde (146 mg, 1.07 mmol) was added to the solution under ice bath. The temperature was allowed to rise to 66 ℃ for 2.0 h. Subsequently, the solution was cooled to room temperature followed by adding 5.0 mL saturated NH_4Cl solution. The solvent was then removed under reduced pressure and the resulting solid was suspended in CH_2Cl_2 (10 mL), washed with H_2O (10 mL). After drying of the organic phase over Na_2SO_4 and evaporation of the solvent, the residue was purified by filtration column (SiO_2, hexane/AcOEt = 5/1, v/v) affording **3e** as pale yellow solid (214 mg, 0.88 mmol, 82%). ^{1}H NMR (400 MHz, Acetone-d_6) δ 7.28 (dd, J = 7.5, 1.6 Hz, 2H), 7.21 (td, J = 8.0, 1.7 Hz, 2H), 6.93 (d, J = 8.1 Hz, 2H), 6.89 (t, J = 7.5 Hz, 2H), 6.41 (d, J = 4.9 Hz, 1H), 4.34 (s, 1H), 3.76 (s, 6H); ^{13}C NMR (101 MHz, Acetone-d_6) δ 157.71, 133.44, 128.82, 128.35, 120.84, 111.31, 65.32, 55.73. ESI-HRMS (m/z) calcd. for $C_{15}H_{16}O_3$ $[M+Na]^+$ 267.2755, found 267.0973.

3 Solubility determination

UV-vis spectra were used to record the percentage of solubilized cytochrome *c* by cyclic host **1** after stirring for 3 h. Host **1** showed no UV absorbance from 390 to 410 nm. One equivalent of cytochrome *c* is well solubilized in the mixture of water and methanol (1/1, v/v), which has nearly no solubility in pure methanol. However, 1000

equivalent of host **1** can make one equivalent of cytochrome *c* be fully solubilized in pure methanol as shown in Fig. S1. This molar ratio (1000:1) was obtained from a UV experiment. To a quantified cytochrome *c* (one equivalent) solution different amounts (from 10 to 1000 equivalents) of host **1** were added and stirred for 3 h in MeOH, then the mixture was determined by UV-vis spectroscopy (Fig. S2). All the results were based on the absorbance at 400 nm and summarized in Table S1. The results show that for one equivalent of cytochrome *c*, 10 equivalents of the host can only solubilize 21% cytochrome *c* and 500 equivalents host can solubilize 92% cytochrome *c*. When the amount of cyclic host reaches 1000 times that of cytochrome *c*, 100% cytochrome *c* can be solubilized. So we choose 1:1000 molar ratio of cytochrome *c* and macrocyclic host to guarantee that the cytochrome *c* added to catalyze the reaction could be fully solubilized in methanol.

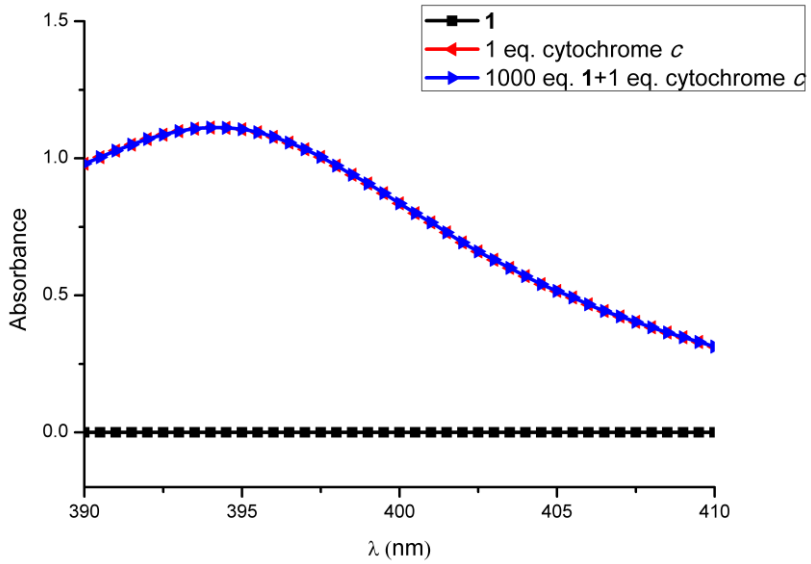

Fig. S1. UV-vis spectra of cytochrome *c* (MeOH/H_2O, 1/1, v/v), cytochrome *c* complex (MeOH) and cyclo[6]aramide **1** (MeOH) from 390 to 410 nm after stirring for 3 h.

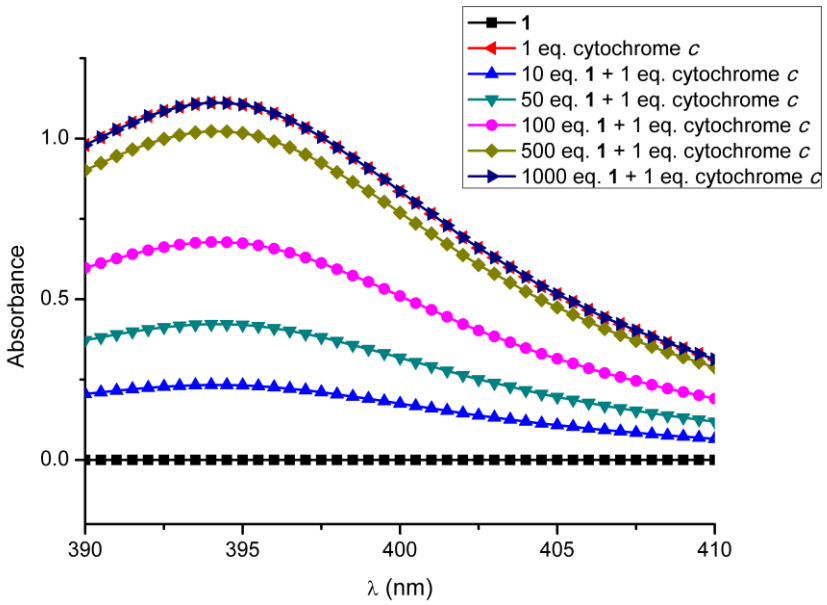

Fig. S2. Determination of solubility of cytochrome *c* with different equivalents of cyclo[6]aramide **1** by UV-vis experiment from 390 to 410 nm after stirring for 3 h in MeOH. The red curve of one cytochrome *c* was determined in the 1:1 mixture of water and methanol as a standard.

Table S1 Solubility of cytochrome *c* after adding cyclo[6]aramide **1** in methanol. The data based on the absorbance at 400 nm.

Concentration of **1** (M)	Equivalent of cytochrome *c*	Equivalent of **1**	Concentration of solubilized cytochrome *c* (M)	Equivalent of solubilized cytochrome *c*	Percentage of solubilized cytochrome *c*
1.0×10^{-4}	1.0 eq.	10 eq.	2.1×10^{-6}	0.21 eq.	21%
5.0×10^{-4}	1.0 eq.	50 eq.	3.8×10^{-6}	0.38 eq.	38%
1.0×10^{-3}	1.0 eq.	100 eq.	6.1×10^{-6}	0.61 eq.	61%
5.0×10^{-3}	1.0 eq.	500 eq.	9.2×10^{-6}	0.92 eq.	92%
1.0×10^{-2}	1.0 eq.	1000 eq.	1.0×10^{-5}	1.00 eq.	100%

4 Characterization of supramolecular complex

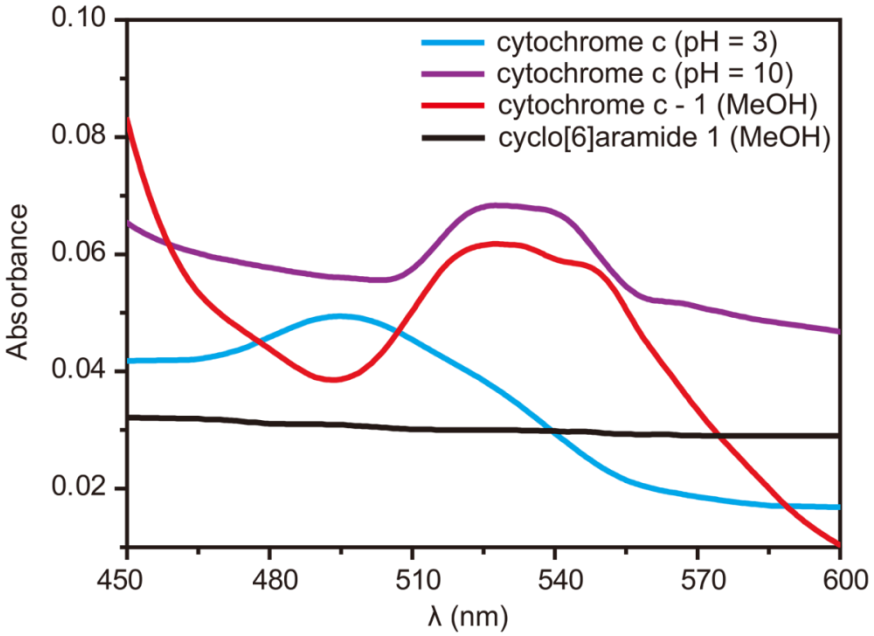

Fig. S3. UV-vis spectra of cytochrome *c* (pH = 3.0), cytochrome *c* (pH = 10.0), cytochrome *c* complex (MeOH) and cyclo[6]aramide **1** (MeOH) from 450 to 600 nm.

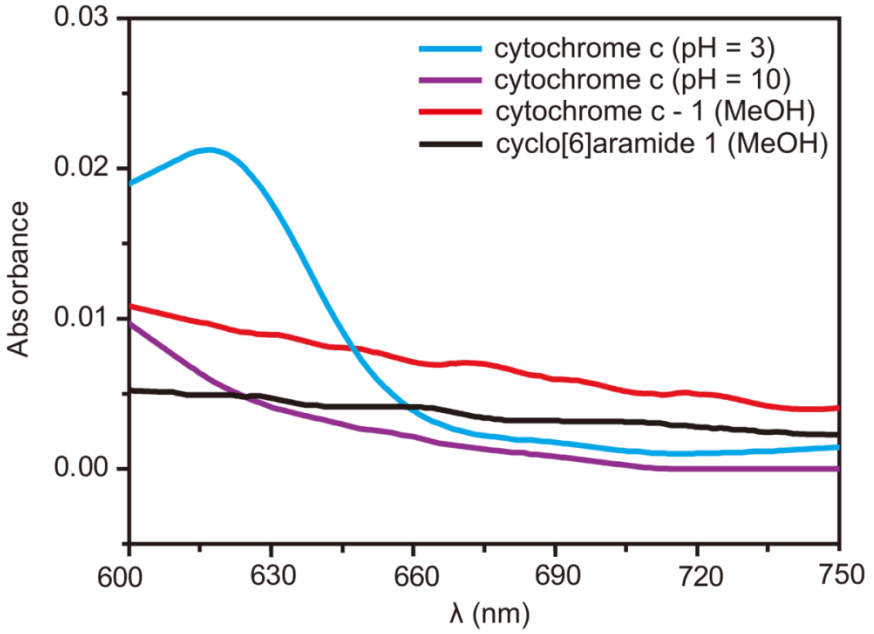

Fig. S4. UV-vis spectra of cytochrome *c* (pH = 3.0), cytochrome *c* (pH = 10.0), cytochrome *c* complex (MeOH) and cyclo[6]aramide **1** (MeOH) from 600 to 750 nm.

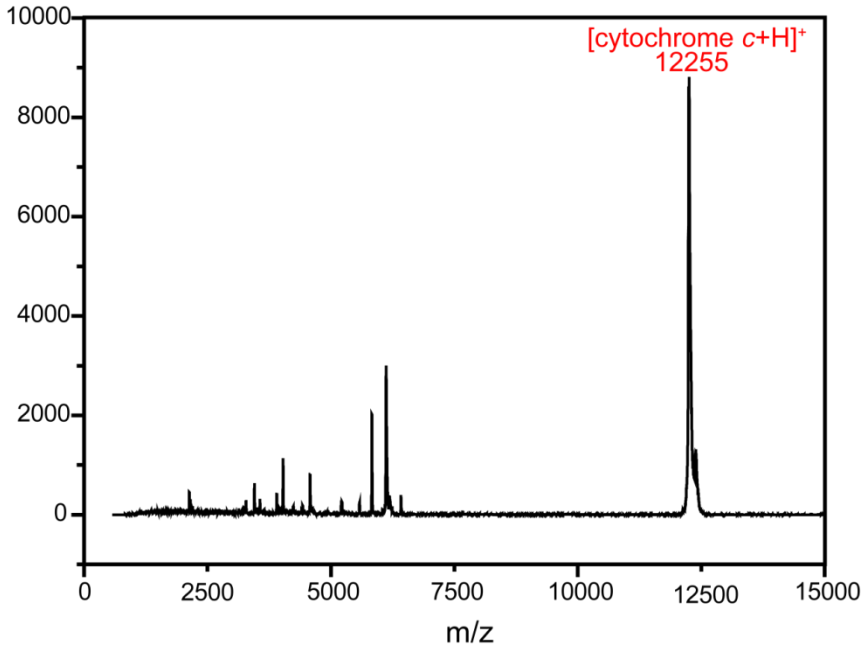

Fig. S5. The MALDI-TOF mass spectrum of cytochrome *c*.

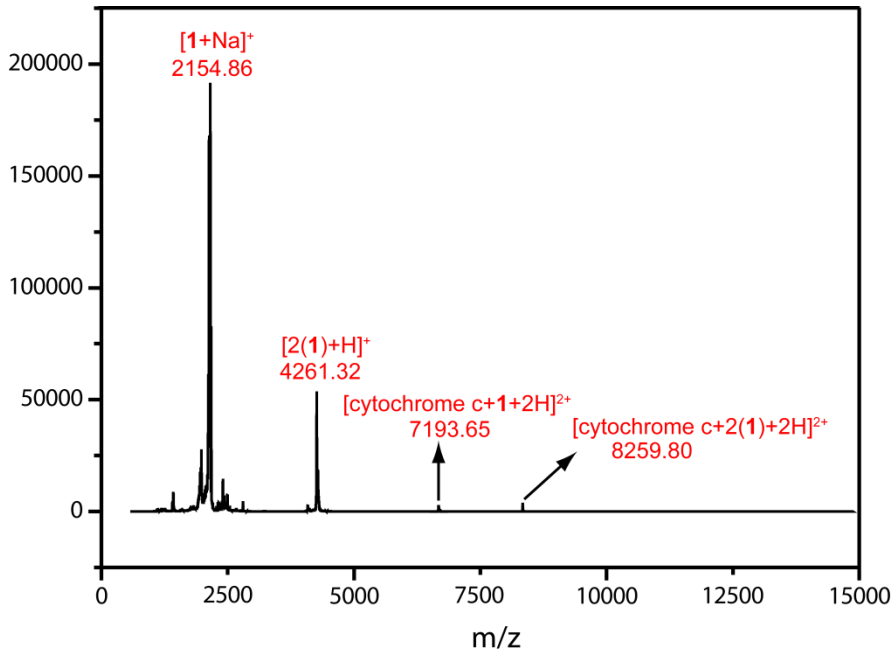

Fig. S6. The MALDI-TOF mass spectrum of complex of cytochrome *c* and host **1**.

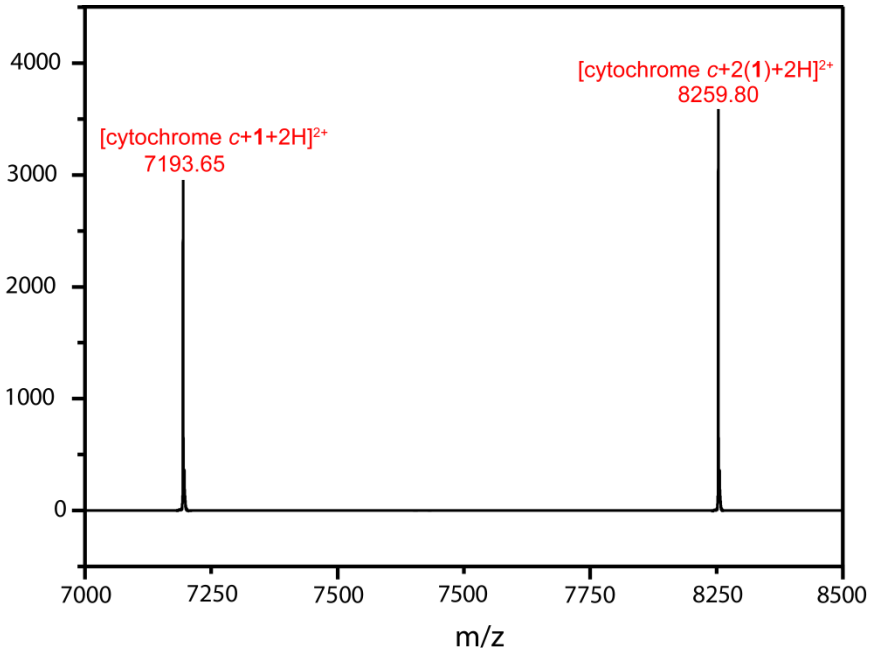

Fig. S7. Partially enlarged MALDI-TOF mass spectrum of complex of cytochrome *c* and host **1**.

5 Computational details

5.1 Distribution of lysine and arginine residues

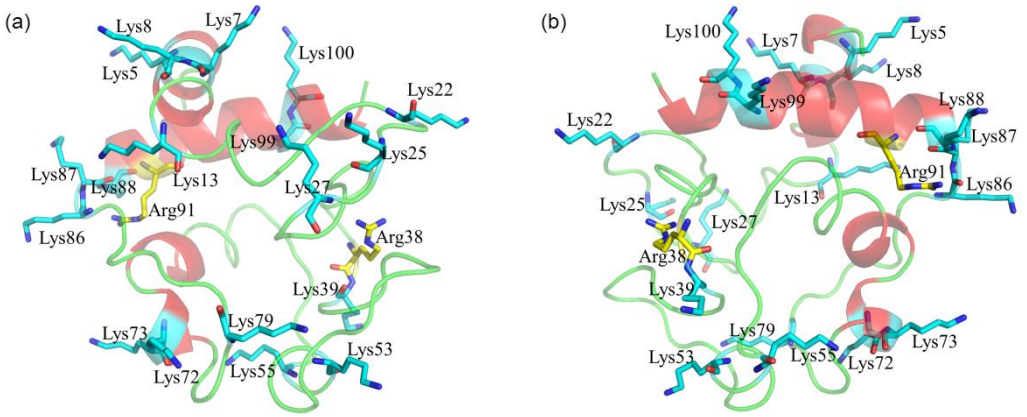

Fig. S8. The cartoon of distribution of lysine residues and arginine residues (showed by stick style) on cytochrome *c* (PDB code 2B4Z). (a) and (b) show the same structure in different views.

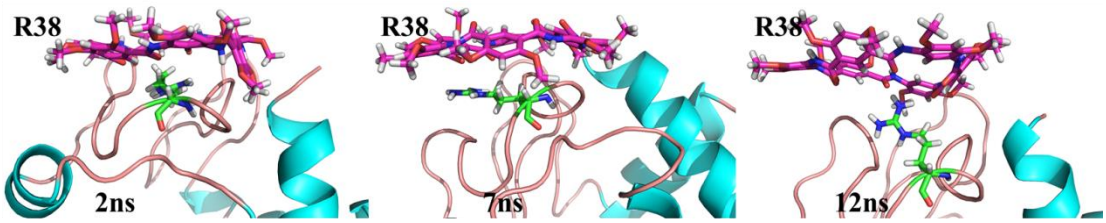

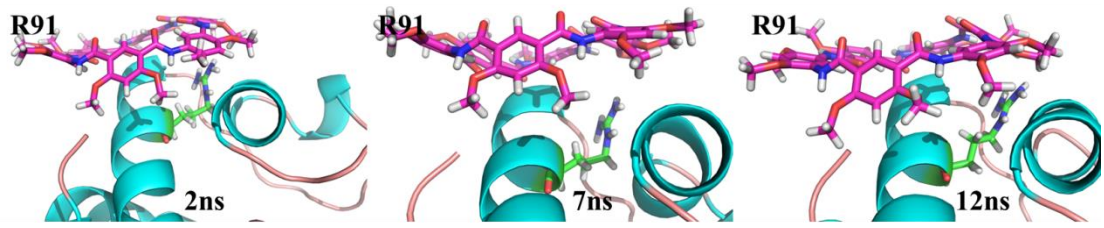

Fig. S9. Snapshots of the binding models along the dynamics simulation time. For clarity, the water molecules have been removed. The arginine residues are plotted using stick style and the cyclo[6]aramide is plotted using stick style, while cartoon style for cytochrome *c*.

5.2 Docking protocol

To simplify our simulations, we first built an analogue model **2** for cyclo[6]aramide with all long side chains replaced with methyl groups. All missing hydrogen atoms were added to cytochrome *c* using leap module implemented in Amber12 program, while hydrogen atoms for cyclo[6]aramide **2** were added using ADT.[S2] The partial charges for both receptor (cytochrome *c*) and macrocyclic ligand (cyclo[6]aramide **2**) were assigned using ADT with Gasteiger method.[S3]

A grid map of 47.25 Å × 47.25 Å × 47.25 Å points with 0.375 Å grid spacing was generated using AutoGrid module based on the center of cytochrome *c*. The Lamarckian genetic algorithm (LGA)[S4] was applied as the searching approach. A total of 12000 automated docking runs were finally generated for a 150 population size with a 2,500,000 maximum number of energy evaluation for each docking experiment. Subsequently, cluster analysis was applied on docked results using a root-mean-square deviation (RMSD) tolerance of 2.0 Å. Then, one docked conformation with the lowest energy in each docking cases was selected as the initial model for further MD simulation and binding free energy calculation.

5.3 Molecule dynamic

The obtained systems were firstly solvated in a pre-equilibrated methanol water box.[S5] The typical size of the methanol box is calculated to be about 75 ± 1 Å × 75 ± 1 Å × 75 ± 1 Å, consisting of 1852 solute atoms and about 1600 ± 200 solvent molecules. First of all, the geometry optimizations of cyclo[6]aramide **2** at HF/6-31G* level of theory were carried out using Gaussian 09 suite of program[S6]. The partial atomic charges were then calculated using the restrained electrostatic potential (RESP) protocol after structure optimization and electrostatic potential calculations using B3LYP/6-31G* method. The force field parameters for the ligands generated using the Antechamber program were then described by GAFF module. The force field of cytochrome *c* is described using AMBER ff99SB parameters, while the force field for hemoglobin was adopted from AMBER parameter database. The periodic boundary conditions (PBC) and a 12 Å cutoff for non-bond interactions were

applied. The particle mesh ewald (PME) algorithm[S7] was used to calculate the long-range electrostatic interactions. The positions of water molecules were relaxed by 5000 steps of steepest descent (SD) and 5000 steps of conjugate gradient (CG) minimization approach with all of solute molecules fixed at their original positions. Further 10,000 steps of CG full minimization were carried out for total system. The obtained systems were gradually heated to 300 K in 50 ps in the NVT ensemble, followed by 50 ps to keep the pressure to 1 atm. After 2 ns equilibration simulation under 1 atm pressure and 300 K, additional 10 ns MD simulations in the isothermal–isobaric ensemble (NPT) were performed for data analysis. Newton's equations of atomic motion were integrated by the Verlet algorithm with a 2-fs time step. SHAKE algorithm[S8] was applied to constraint bond stretching of the covalent bonds involving hydrogen atoms. All of MD simulations were performed using Sander module implemented in AMBER 12 software package.

5.4 Binding free energy calculations

To quantitatively assess the binding affinity of cytochrome *c* in complex with cyclo[6]aramide molecule, it is necessary to calculate the binding free energy for the inclusion complex. In this work, the binding free energy is calculated using MM-GBSA method.[S9]

For the calculation of binding free energy in MM-GBSA framework, it has been discussed extensively.

$$\Delta G_{binding} = \Delta G_{complex} - \Delta G_{pretein} - \Delta G_{ligand} \quad (1)$$

$$\mathrm{G} = G_{gas} + G_{sol} - TS \quad (2)$$

$$E_{gas} = E_{int} + E_{vdw} + E_{ele} \quad (3)$$

$$G_{sol} = G_{GB} + G_{np} \quad (4)$$

$\Delta G_{complex}$, $\Delta G_{pretein}$and$\Delta G_{ligand}$are free energies of the complex, the cytochrome *c* and cyclo[6]aramide **2**, respectively. Each term can be obtained according to Eq. (2). Practically, they are calculated as the statistical averages over frames extracted from MD trajectories. The solvation free energy (G_{sol}) can be divided into polar (G_{GB}) and nonpolar (G_{np}) contributions. The polar solvation contribution is calculated by solving the Generalized Born (GB) equation.[S10] The nonpolar contribution due to cavity formation and van der Waals interactions between the solute and the solvent can be estimated by the equation of $\gamma \cdot SA + b$, where γ = 0.0072 kcal/Å^2, b = 0.0 kcal/mol. The SA is defined as the solvent accessible surface area, which was estimated using the program MSMS.[S11] For each complex system, binding energies were averaged over 1,000 frames of the 10 ns MD trajectory. It has long been recognized that the inclusion of entropic effect in the calculation of total binding free energy can largely reduce the difference. Entropy contributions are from changes in the degrees of freedom including translation, rotation and vibration. The translational, rotational and vibrational entropy terms are functions of the mass and moments of inertia of the

molecule and thus can be calculated using the standard equations of statistical mechanics. In this work, vibrational entropy contributions were estimated using the analysis approach. Due to large system size, the $-T\Delta S$ was averaged over 10 snapshots of the MD trajectory.

5.5 Center of mass distance

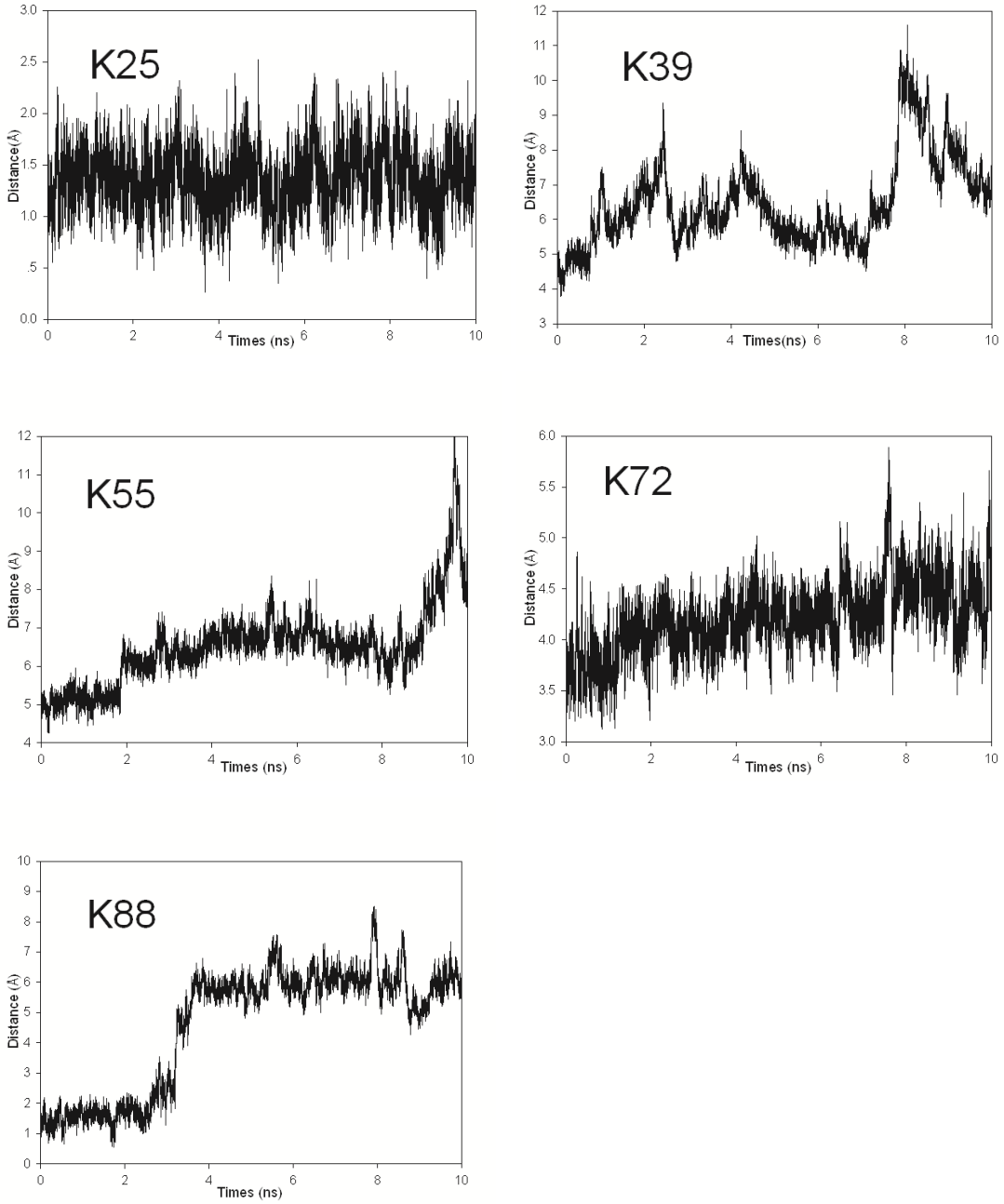

Fig. S10. The center of mass distance between the cyclo[6]aramide **2** and residues of cytochrome *c* along the simulation time.

5.6 Binding models

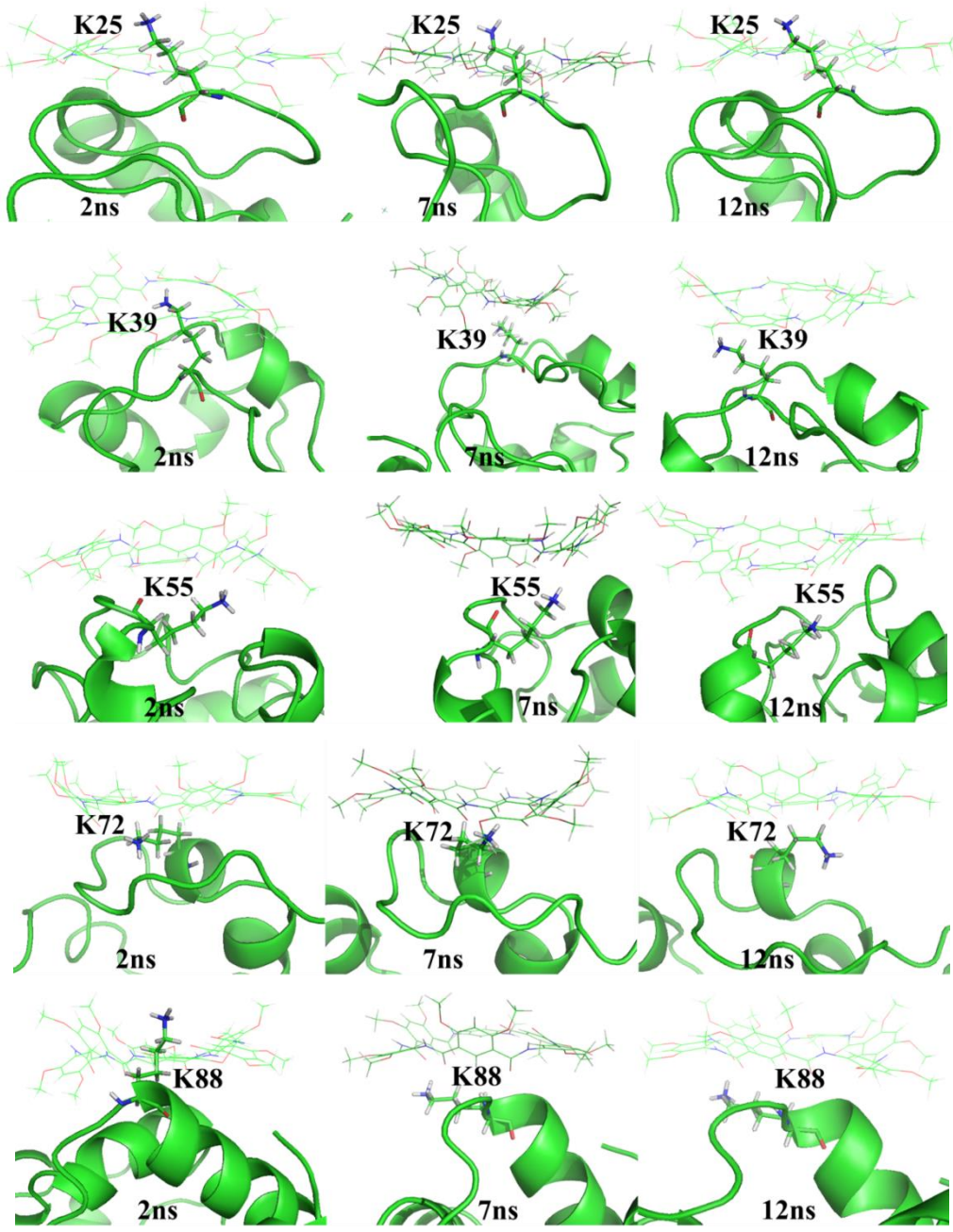

Fig. S11. Snapshots of the binding models along the dynamics simulation time. For clarity, the water molecules have been removed. The lysine residues are plotted using stick style and the cyclo[6]aramide **2** is plotted using line style, while cartoon style for cytochrome *c*.

6 Yield of oxidation reaction

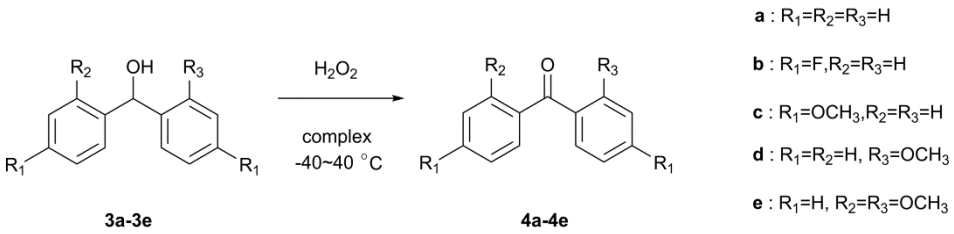

Scheme S3. Catalytic oxidation reaction of substrates: **3a** benzhydrol; **3b** 4,4'-difluorobenzhydrol; **3c** 4,4'-dimethoxybenzhydrol; **3d** 2-methoxyphenyl(phenyl)methanol; **3e** dis(2-methoxyphenyl)methanol.

The reaction mixture 3.0 mL comprises 4.00×10^{-4} mol/L substrate (benzhydrol derivative **3a**-**3e**) and 1.00×10^{-4} mol/L cytochrome *c*-cyclo[6]aramide **1** complex (1:1000 cytochrome *c*/**1**) in methanol. The oxidation experiments were carried out with the above reaction mixture at various temperatures with addition of 8.00×10^{-4} mol/L hydrogen peroxide to start the reaction. The reaction is completed in 4 h. After centrifugal filtration, the reaction solution was analyzed by HPLC technique: Diamonsil C18, 25 ℃, H_2O/methanol = 3/7, 1.0 mL/min. The yields were obtained with the equation below:

$$\text{yield}\% = \frac{A_p}{A_t} \times 100\%$$

In this equation, A_p represents the practical peak area after the reaction determined by HPLC, and A_t refers to the theoretical peak area dependent on the concentration of products **4a**-**4e**.

Taking **4a** as an example, a standard curve was prepared for **4a** using a series of concentrations from 1.00×10^{-4} mol/L to 10.00×10^{-4} mol/L by external standard method according to peak areas in HPLC traces. From the standard curve, the theoretical area A_t at the concentration of 4.00×10^{-4} mol/L was obtained. The recovered reaction mixture of **3a** was then determined under the same HPLC condition, and the peak area of **4a** denoted as A_p in HPLC trace was thus achieved. Finally, the yield was calculated via the equation above.

Table S2 Yields of **4a**-**4e** in the presence of H_2O_2 with cytochrome *c*-cyclo[6]aramide **1** complexes as the catalyst

Products	-40 ℃	-20 ℃	0 ℃	20 ℃	40 ℃
4a	43.0 %	25.3 %	17.5 %	11.9 %	9.8 %

4b	36.2 %	26.9 %	17.1 %	11.3 %	8.5 %
4c	45.5 %	25.2 %	17.6 %	12.1 %	4.6 %
4d	23.3 %	20.0 %	6.1 %	<1 %	<1 %
4e	16.1 %	5.3 %	<1 %	<1 %	<1 %

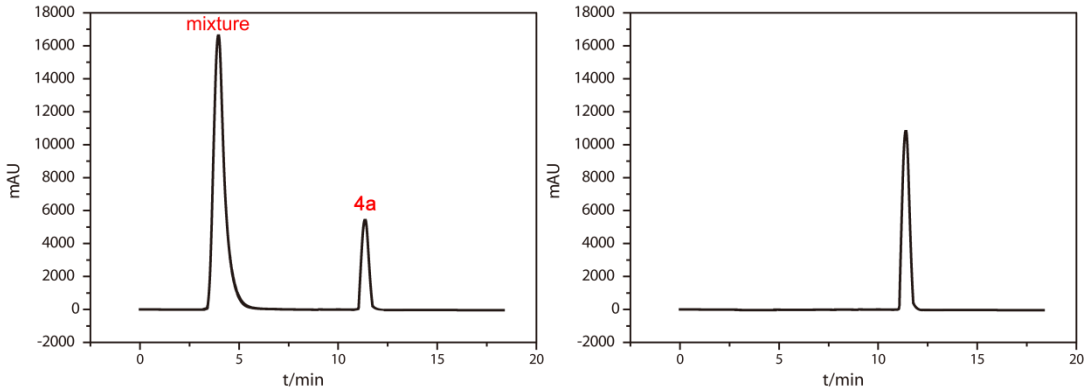

Fig. S12. HPLC (Diamonsil C18, 25 ℃, H_2O/methanol = 3/7, 1.0 mL/min) traces for the reaction (left) of substrate **3a** in the presence of cytochrome *c* complex at -40 ℃ and pure product **4a** (right). "Mixture" denotes the peak from cytochrome *c*-cyclo[6]aramide **1** complex, **3a** and H_2O_2, each of which appears with the same retention time (see Fig. S17, S22 and S23).

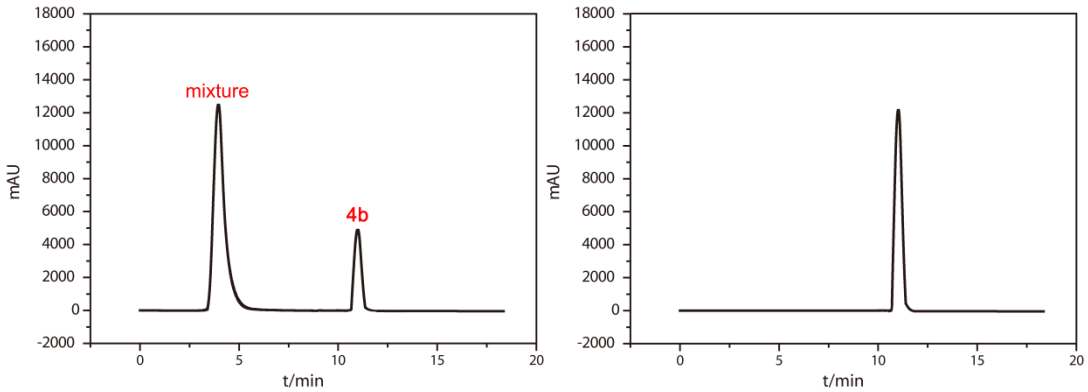

Fig. S13. HPLC (Diamonsil C18, 25 ℃, H_2O/methanol = 3/7, 1.0 mL/min) traces for the reaction (left) of substrate **3b** in the presence of cytochrome *c* complex at -40 ℃ and pure product **4b** (right). "Mixture" denotes the peak from cytochrome *c*-cyclo[6]aramide **1** complex, **3b** and H_2O_2, each of which appears with the same retention time (see Fig. S18, S22 and S23).

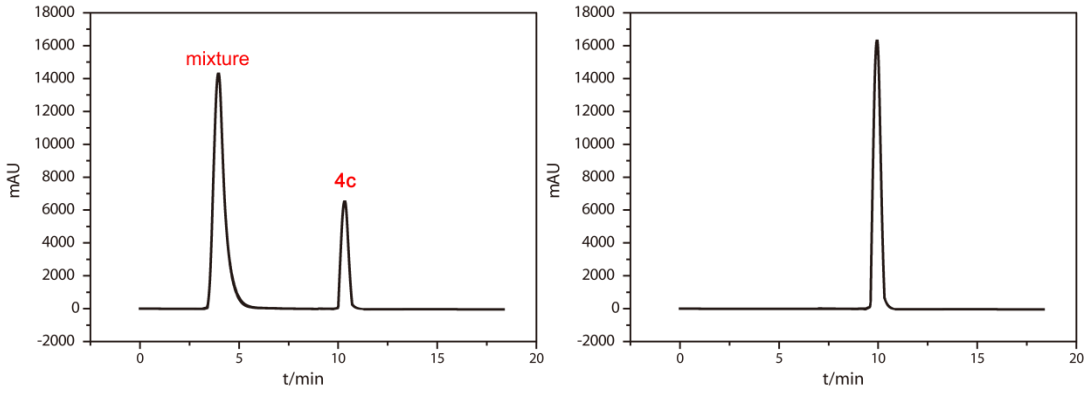

Fig. S14. HPLC (Diamonsil C18, 25 ℃, H_2O/methanol = 3/7, 1.0 mL/min) traces for the reaction (left) of substrate **3c** in the presence of cytochrome *c* complex at -40 ℃ and pure product **4c** (right). "Mixture" denotes the peak from cytochrome *c*-cyclo[6]aramide **1** complex, **3c** and H_2O_2, each of which appears with the same retention time (see Fig. S19, S22 and S23).

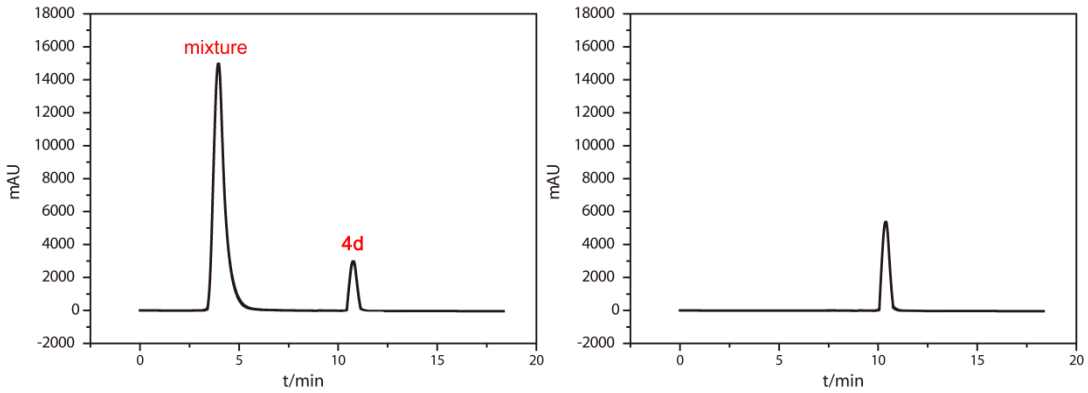

Fig. S15. HPLC (Diamonsil C18, 25 ℃, H_2O/methanol = 3/7, 1.0 mL/min) traces for the reaction (left) of substrate **3d** in the presence of cytochrome *c* complex at -40 ℃ and pure product **4d** (right). "Mixture" denotes the peak from cytochrome *c*-cyclo[6]aramide **1** complex, **3d** and H_2O_2, each of which appears with the same retention time (see Fig. S20, S22 and S23).

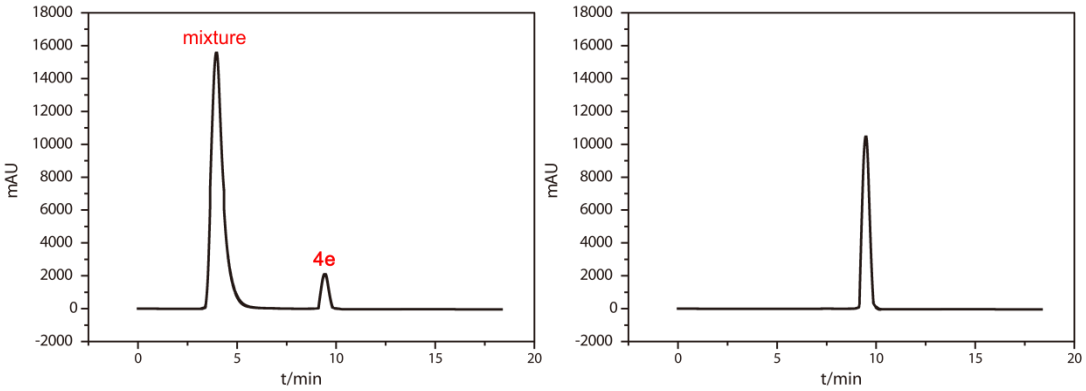

Fig. S16. HPLC (Diamonsil C18, 25 ℃, H_2O/methanol = 3/7, 1.0 mL/min) traces for the reaction (left) of substrate **3e** in the presence of cytochrome *c* complex at -40 ℃ and pure product **4e** (right). "Mixture" denotes the peak from cytochrome *c*-cyclo[6]aramide **1** complex, **3e** and H_2O_2, each of which appears with the same retention time (see Fig. S21, S22 and S23).

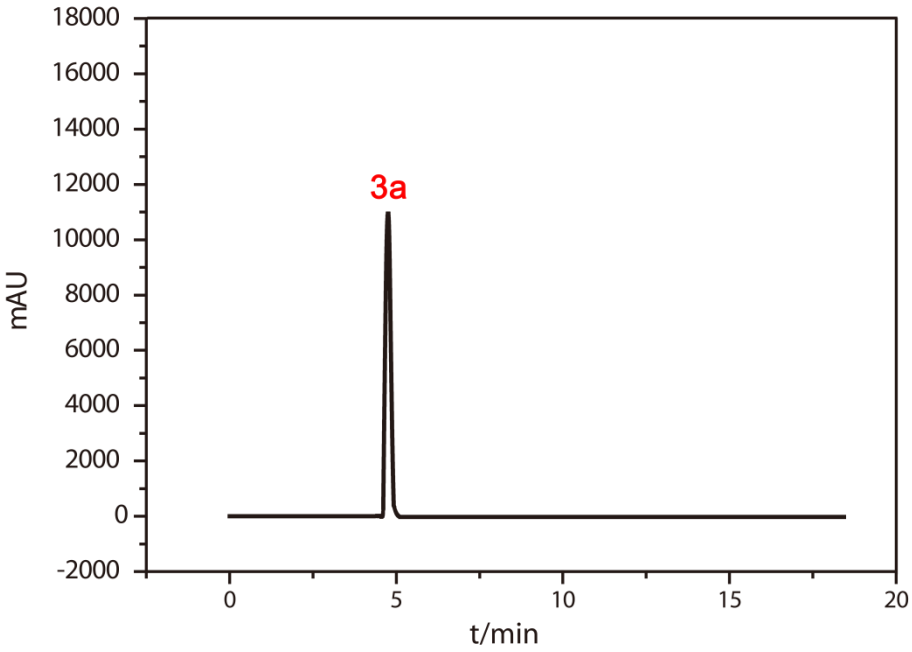

Fig. S17. HPLC (Diamonsil C18, 25 ℃, H_2O/methanol = 3/7, 1.0 mL/min) trace of pure substrate **3a**.

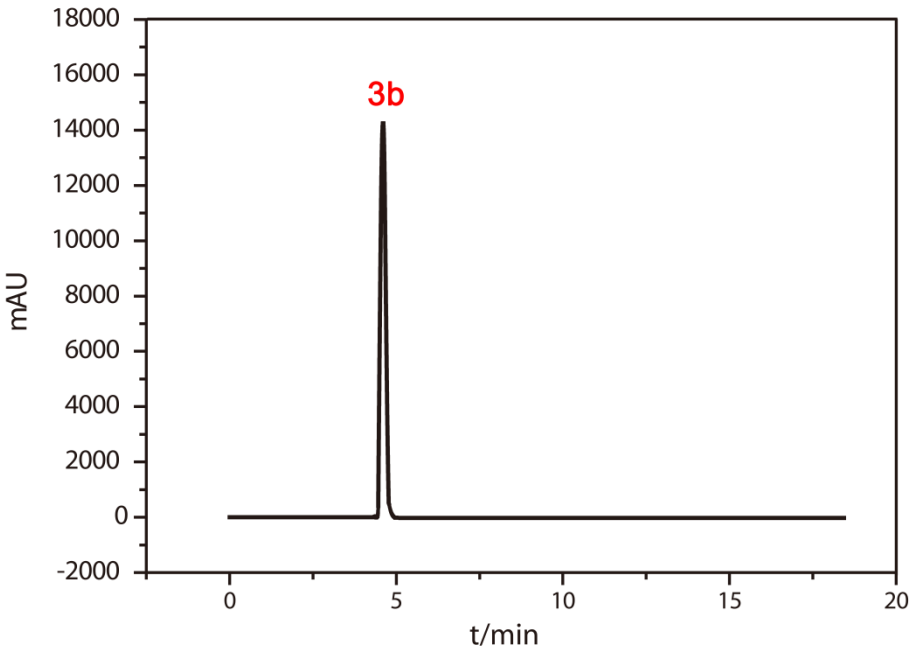

Fig. S18. HPLC (Diamonsil C18, 25 ℃, H_2O/methanol = 3/7, 1.0 mL/min) trace of pure substrate **3b**.

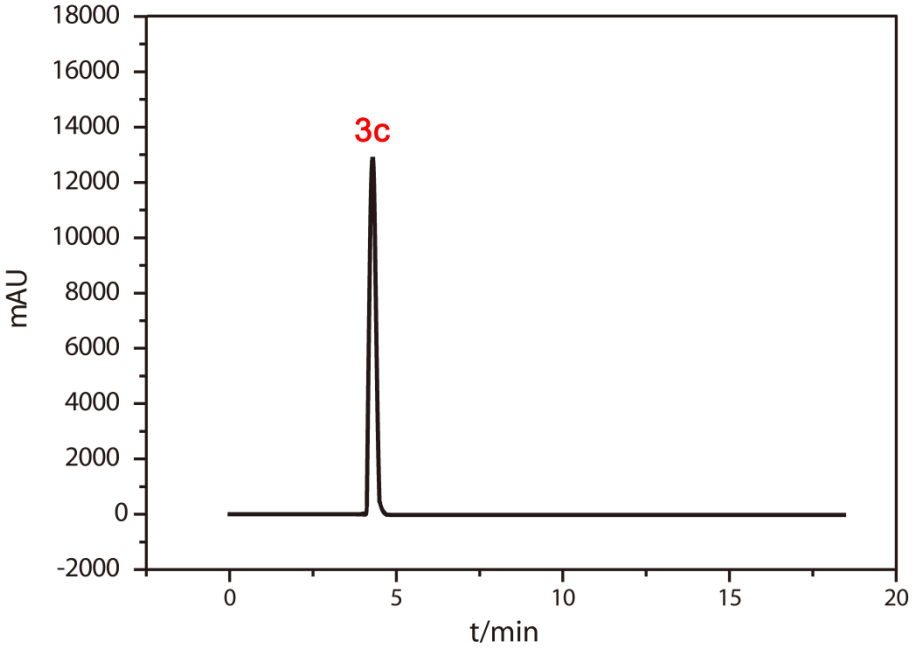

Fig. S19. HPLC (Diamonsil C18, 25 ℃, H_2O/methanol = 3/7, 1.0 mL/min) trace of pure substrate **3c**.

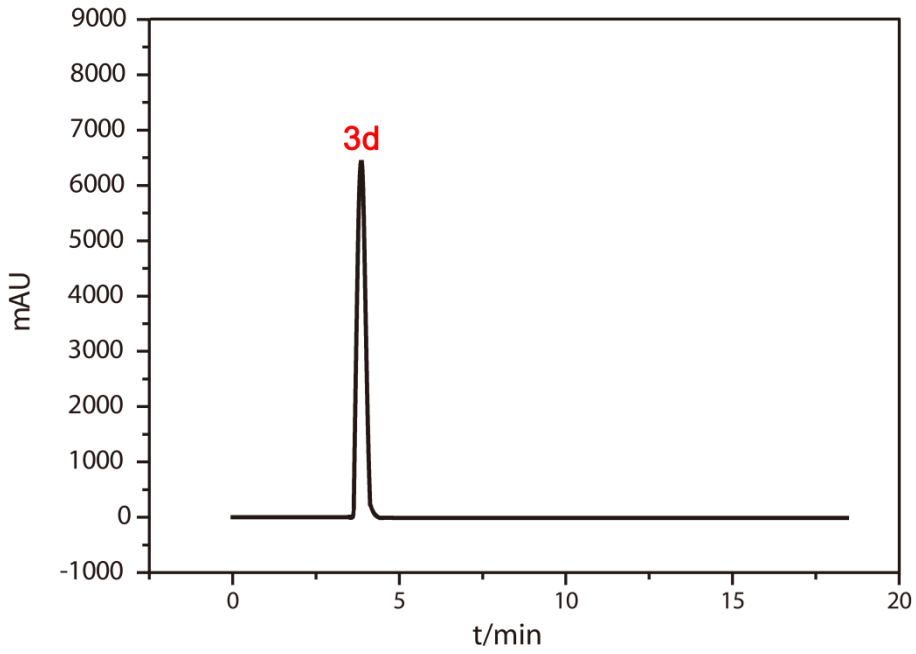

Fig. S20. HPLC (Diamonsil C18, 25 ℃, H_2O/methanol = 3/7, 1.0 mL/min) trace of pure substrate **3d**.

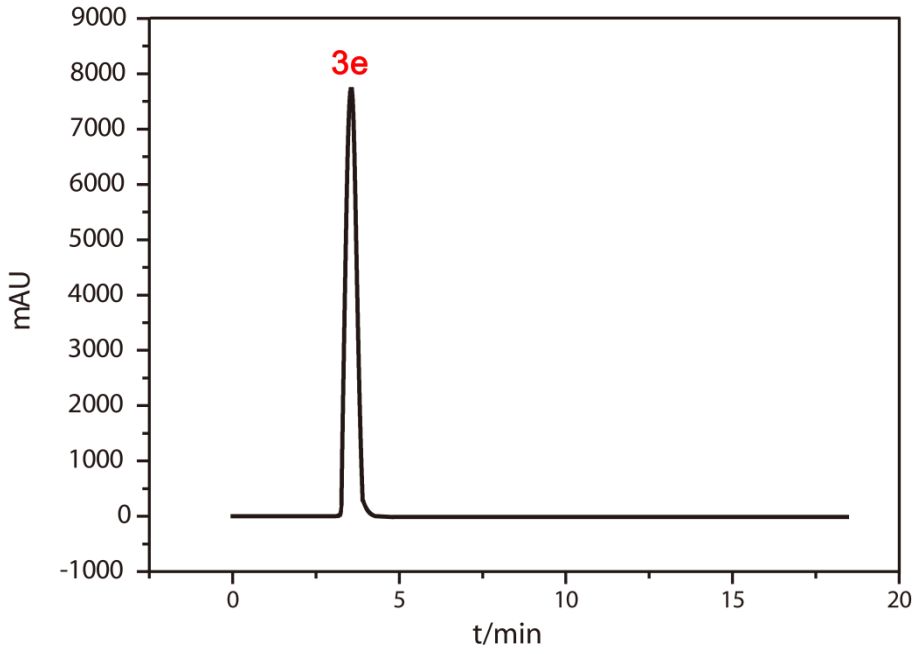

Fig. S21. HPLC (Diamonsil C18, 25 ℃, H_2O/methanol = 3/7, 1.0 mL/min) trace of pure substrate **3e**.

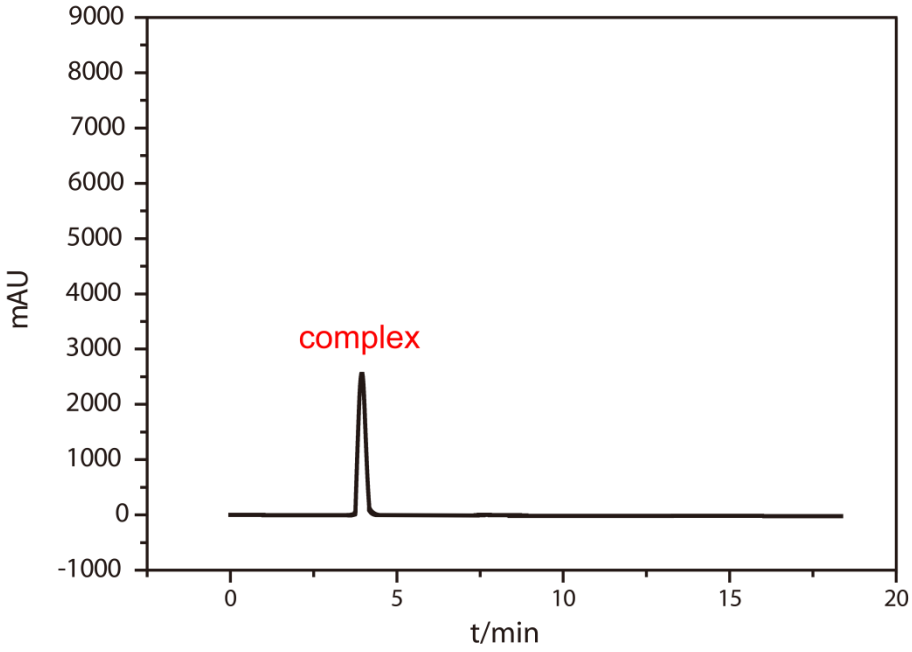

Fig. S22. HPLC (Diamonsil C18, 25 ℃, H_2O/methanol = 3/7, 1.0 mL/min) trace of cytochrome *c*-cyclo[6]aramide **1** complex.

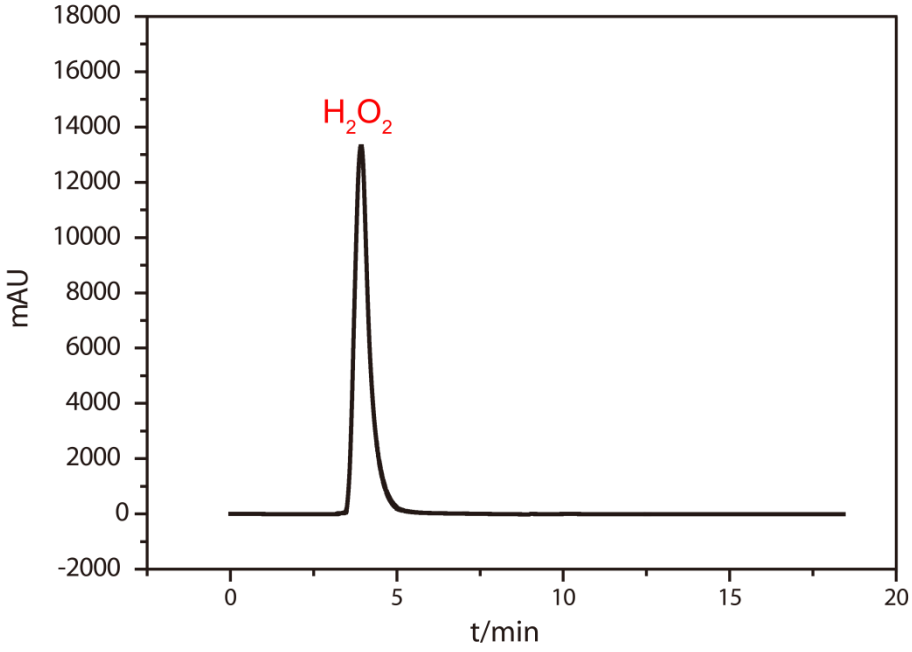

Fig. S23. HPLC (Diamonsil C18, 25 ℃, H_2O/methanol = 3/7, 1.0 mL/min) trace of H_2O_2.

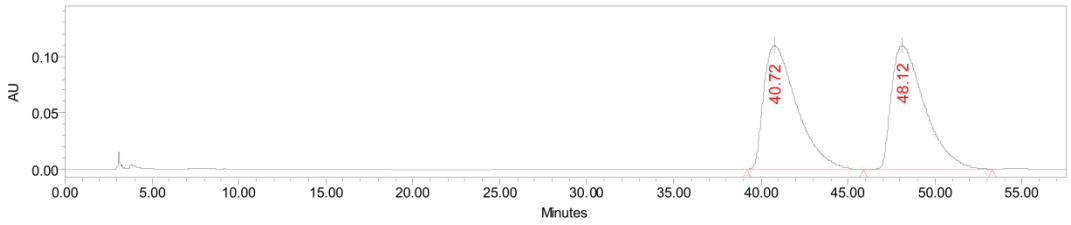

Fig. S24. The HPLC trace (HPLC DAICEL CHIRALCEL AS-H, n-hexane/2-propanol = 90/10, flow rate = 1.0 mL/min, λ = 210 nm) of substrate **3d** before catalytic reaction.

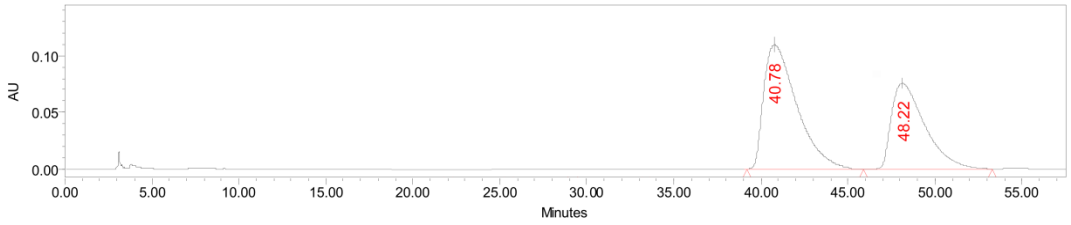

Fig. S25. The HPLC trace (HPLC DAICEL CHIRALCEL AS-H, n-hexane/2-propanol = 90/10, flow rate = 1.0 mL/min, λ = 210 nm) of substrate **3d** after catalytic reaction at 0 ℃. (The enantiomeric excess is 20.3%)

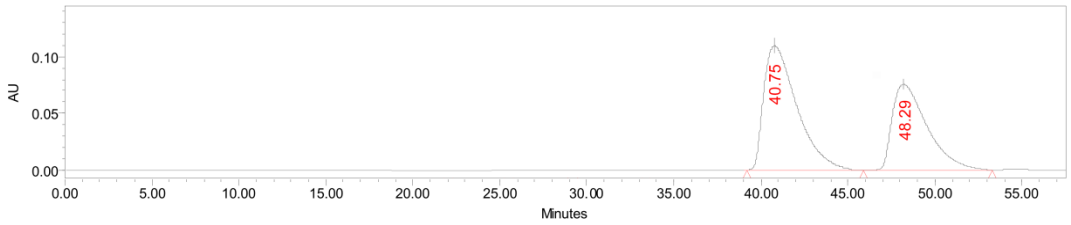

Fig. S26. The HPLC trace (HPLC DAICEL CHIRALCEL AS-H, n-hexane/2-propanol = 90/10, flow rate = 1.0 mL/min, λ = 210 nm) of substrate **3d** after catalytic reaction at -20 ℃. (The enantiomeric excess is 19.3%)

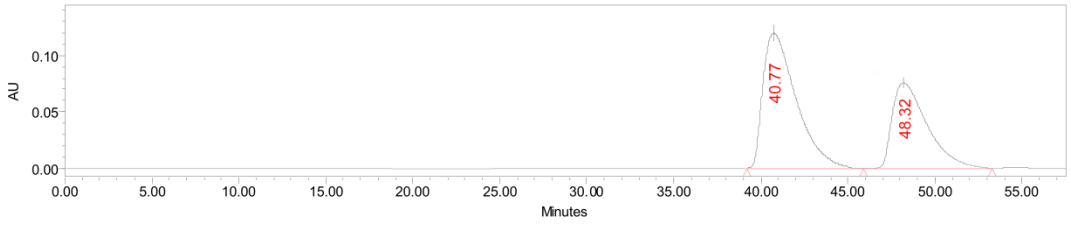

Fig. S27. The HPLC trace (HPLC DAICEL CHIRALCEL AS-H, n-hexane/2-propanol = 90/10, flow rate = 1.0 mL/min, λ = 210 nm) of substrate **3d** after catalytic reaction at -40 ℃. (The enantiomeric excess is 22.6%)

7 Characterization of compounds 3d and 3e

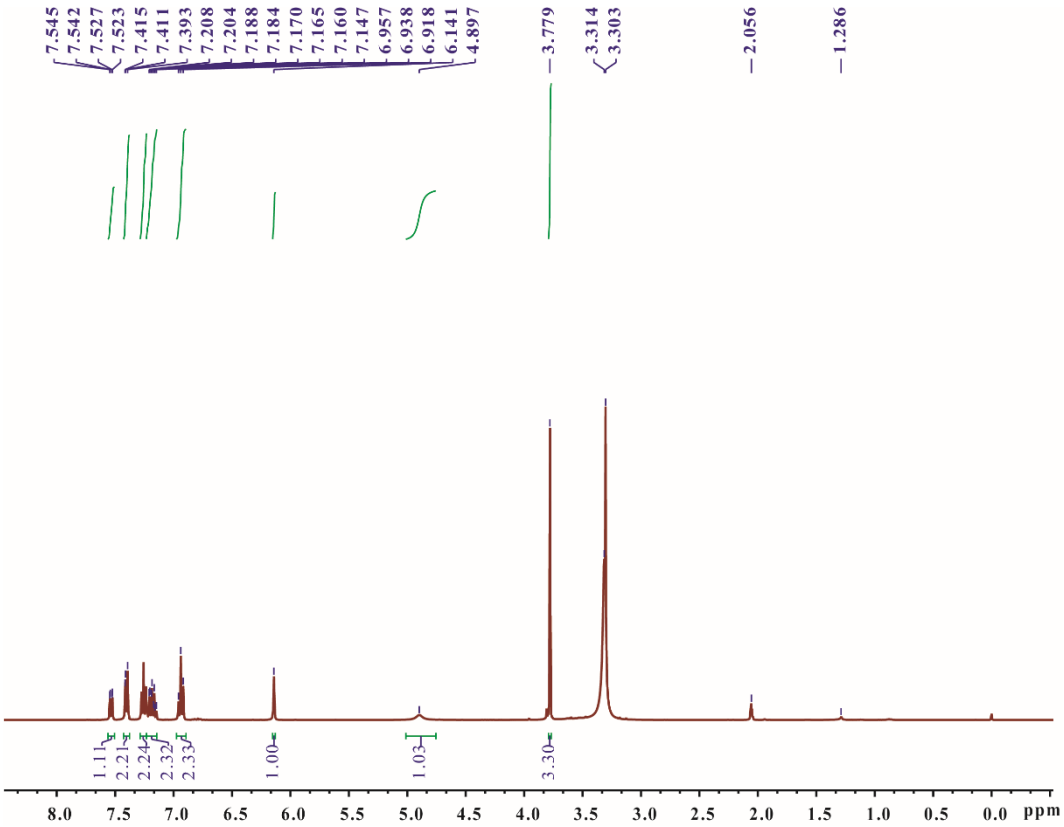

Fig. S28. ^{1}H NMR (400 MHz, CD_3COCD_3, 298 K) spectrum of compound **3d**.

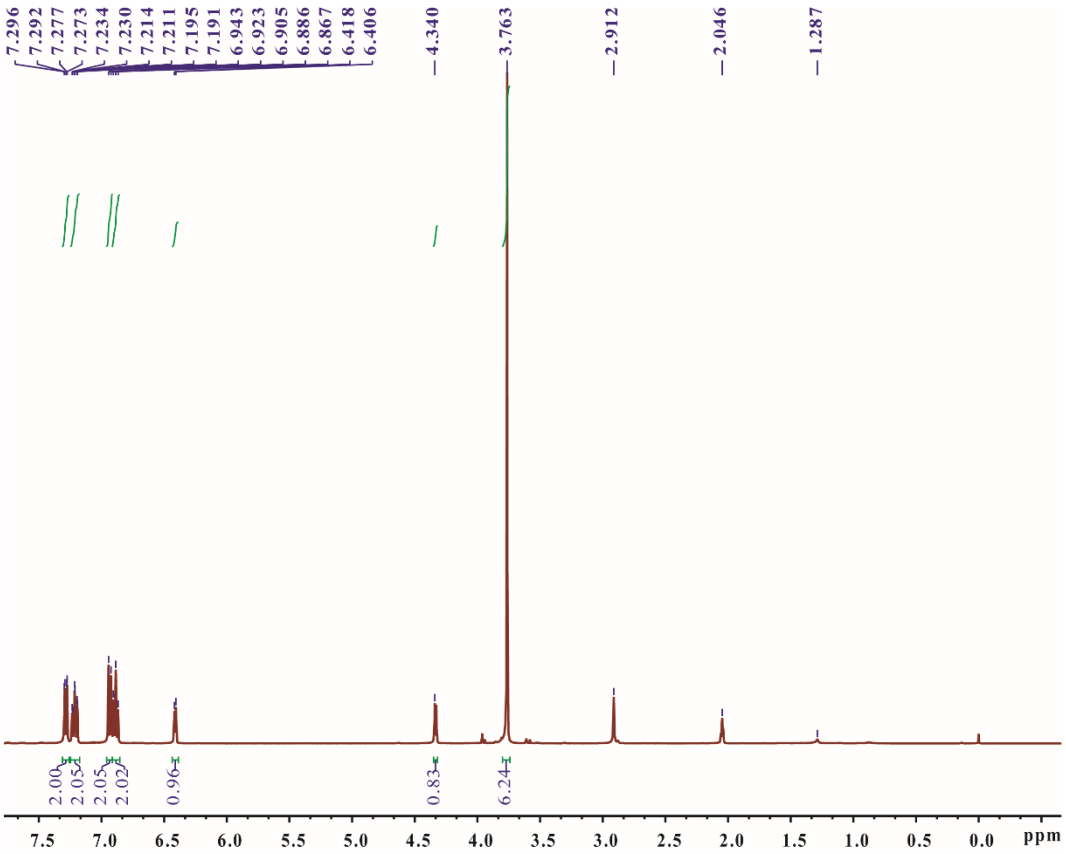

Fig. S29. ^{1}H NMR (400 MHz, CD_3COCD_3, 298 K) spectrum of compound **3e**.

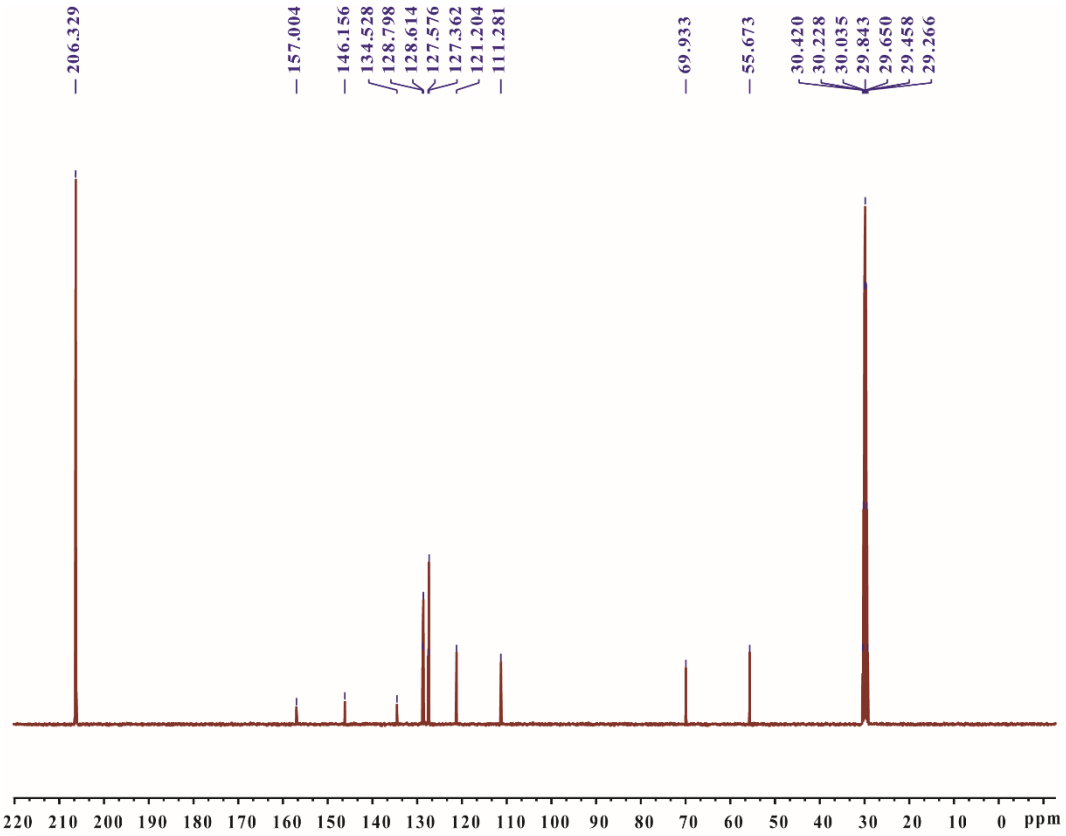

Fig. S30. ^{13}C NMR (400 MHz, CD_3COCD_3, 298 K) spectrum of compound **3d**.

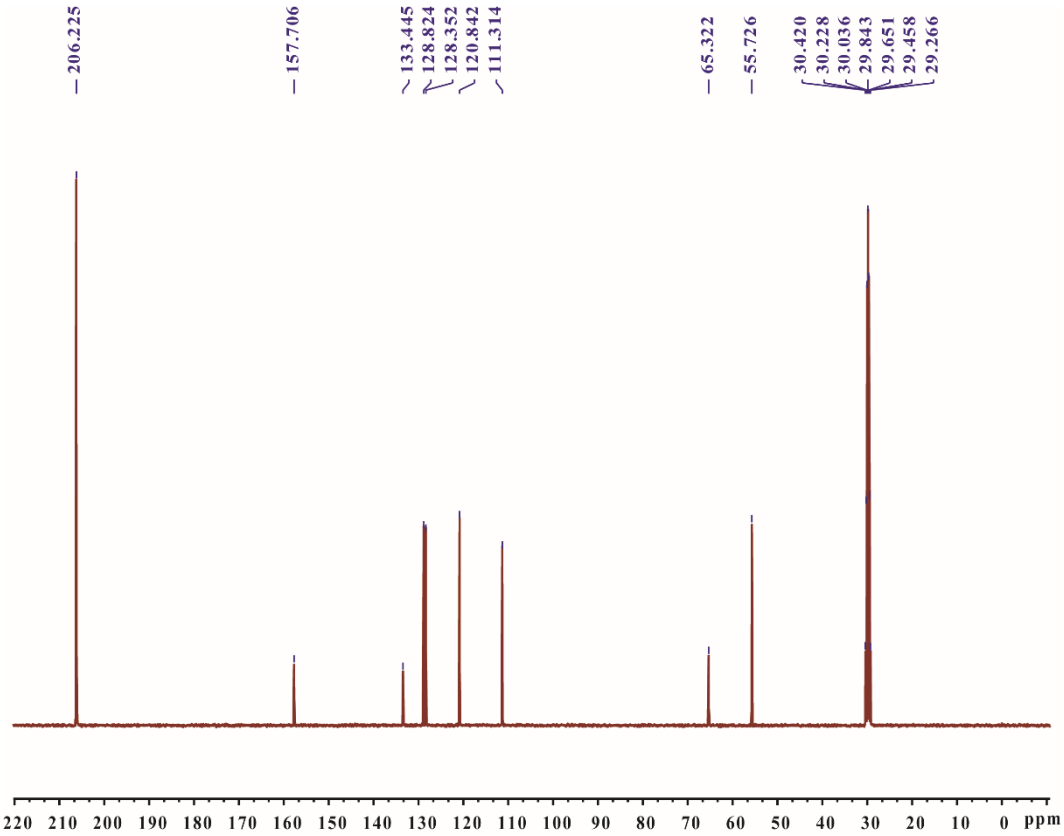

Fig. S31. ^{13}C NMR (400 MHz, CD_3COCD_3, 298 K) spectrum of compound **3e**.

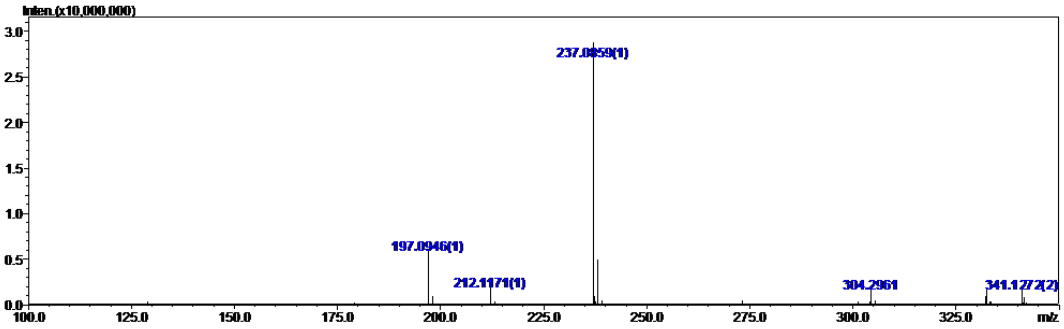

Fig. S32. ESI-HRMS spectrum of compound **3d.**

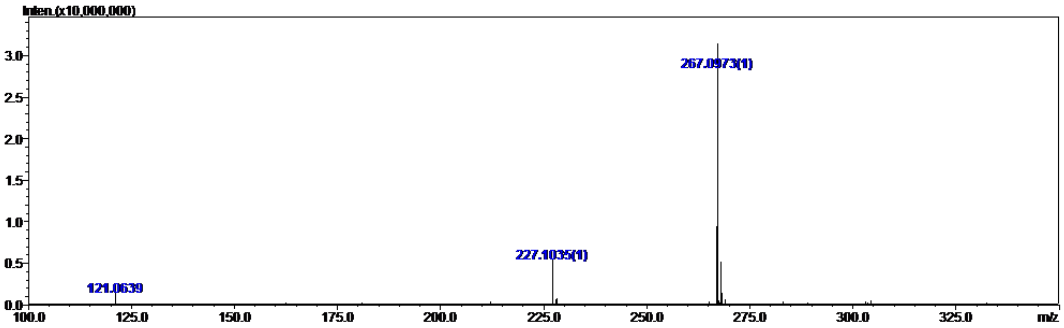

Fig. S33. ESI-HRMS spectrum of compound **3e.**

8 References

S1 Y. He, M. Xu, R. Gao, X. Li, F. Li, X. Wu, D. Xu, H. Zeng and L. Yuan, *Angew. Chem.*, 2014, **126**, 12028-12033.

S2 M. F. Sanner, J. *Mol. Graph. Model.*, 1999, **17**, 57-61.

S3 J. Gasteiger and M. Marsili, *Tetrahedron*, 1980, **36**, 3219-3228.

S4 J. Fuhrmann, A. Rurainski, H.-P. Lenhof and D. Neumann, *J. Comp. Chem.*, 2010, **31**, 1911-1918.

S5 P. Cieplak, J. Caldwell and P. Kollman, *J. Comp. Chem.*, 2001, **22**, 1048-1057.

S6 Gaussian 09, Revision B.01, Frisch, M.J.; Trucks, G. W.; H. B. Schlegel, G. E. Scuseria, M.A. Robb, J. R. Cheeseman, G. Scalmani, V. Barone, B. Mennucci, G.A. Petersson, H. Nakatsuji, M. Caricato, Li, X.; H. P. Hratchian, A. F. Izmaylov, J. Bloino, G. Zheng, J. L. Sonnenberg, M. Hada, M. Ehara, K. Toyota, R. Fukuda, J. Hasegawa, M. Ishida, T. Nakajima, Y. Honda, O. Kitao, H. Nakai, T. Vreven, J. A. Jr. Montgomery, J. E. Peralta, F. Ogliaro, M. Bearpark, J. J. Heyd, E. Brothers, K. N. Kudin, V. N. Staroverov, T. Keith, R. Kobayashi, J. Normand, K. Raghavachari,; A. Rendell, J. C. Burant, S. S. Iyengar, J. Tomasi, M. Cossi, N. Rega, J. M. Millam, M. Klene, J. E. Knox, J. B. Cross, V. Bakken, C. Adamo, J. Jaramillo, R. Gomperts, R. E. Stratmann, O. Yazyev, A. J. Austin, R. Cammi, C. Pomelli, J. W. Ochterski, R. L. Martin, K. Morokuma, V. G. Zakrzewski, G. A. Voth, P. Salvador, J. J. Dannenberg, S. Dapprich, A. D. Daniels, O. J. Farkas, B. Foresman, J. V. Ortiz, J. Cioslowski, Fox, D. J. Gaussian, Inc., Wallingford CT, 2010.

S7 T. Darden, D. York and L. Pedersen, *J. Chem. Phys.*, 1993, **98**, 10089-10092.

S8 J.-P. Ryckaert, G. Ciccotti and H. J. C. Berendsen, *J. Comp. Phys.*, 1977, **23**, 327-341.

S9 J. Srinivasan, T. E. Cheatham, P. Cieplak, P. A. Kollman and D. A. Case, *J. Am. Chem. Soc.*, 1998, **120**, 9401-9409.

S10 A. Onufriev, D. Bashford and D. A. Case, *J. Phy. Chem. B*, 2000, **104**, 3712-3720.

S11 M. F. Sanner, A. J. Olson and J.-C. Spehner, *Biopolymers*, 1996, **38**, 305-320.